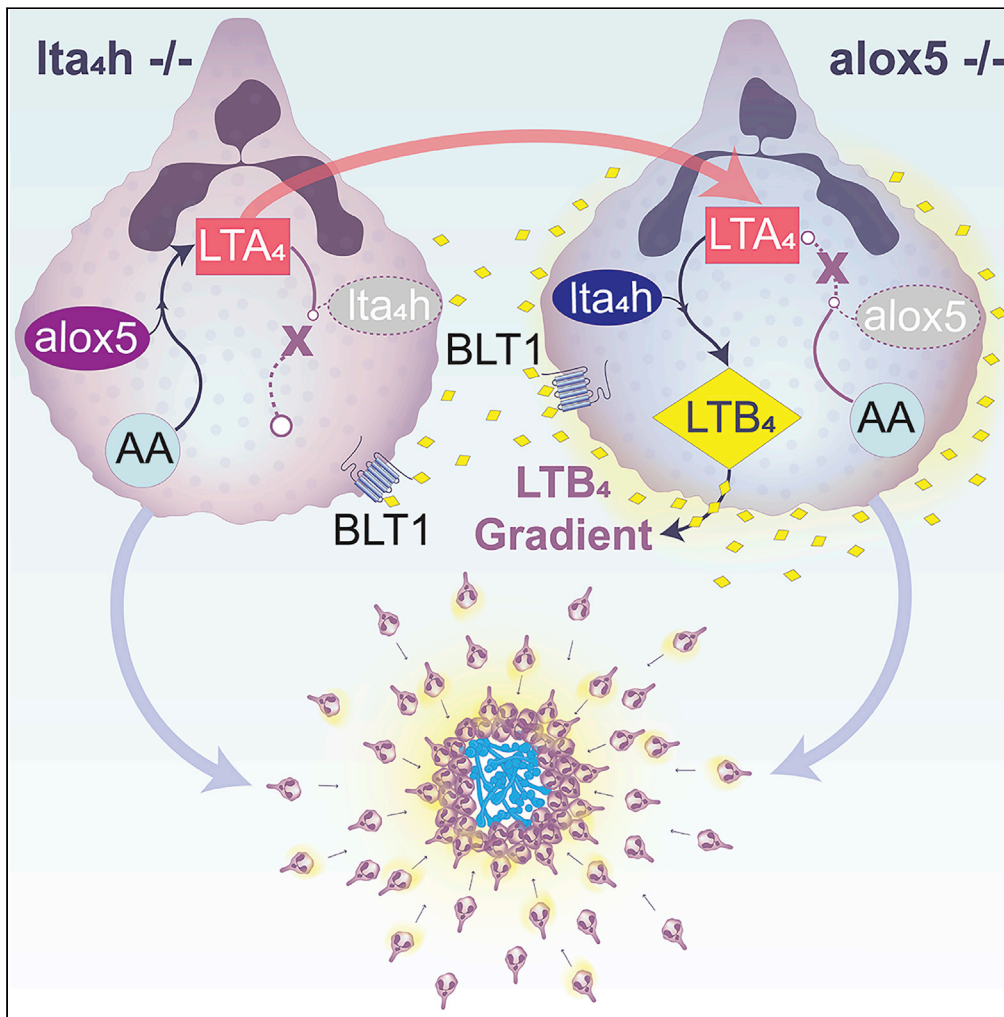


Article

Transcellular biosynthesis of leukotriene B₄ orchestrates neutrophil swarming to fungi



Alex Hopke, Tian Lin, Allison K. Scherer, ..., Charles N. Serhan, Daniel Irimia, Bryan P. Hurley

dirimia@mgh.harvard.edu (D.I.)
bphurley@mgh.harvard.edu (B.P.H.)

Highlights

Mouse neutrophils unable to biosynthesize LTB₄ fail to swarm or contain fungi

Exogenous LTB₄ restores phagocytosis and ROS production but not swarming

Transcellular LTB₄ biosynthesis restores swarming

Transcellular LTB₄ biosynthesis controls fungal growth

Hopke et al., iScience 25, 105226
October 21, 2022 © 2022 The Authors.
<https://doi.org/10.1016/j.isci.2022.105226>



Article

Transcellular biosynthesis of leukotriene B₄ orchestrates neutrophil swarming to fungi

Alex Hopke,^{1,2,3,7} Tian Lin,^{2,4,7} Allison K. Scherer,^{2,5} Ashley E. Shay,^{2,6} Kyle D. Timmer,⁵ Brittany Wilson-Mifsud,⁴ Michael K. Mansour,^{2,5} Charles N. Serhan,^{2,6} Daniel Irimia,^{1,2,3,*} and Bryan P. Hurley^{2,4,8,*}

SUMMARY

Neutrophil swarming is an emergent host defense mechanism triggered by targets larger than a single neutrophil's capacity to phagocytose. Swarming synergizes neutrophil functions, including chemotaxis, phagocytosis, and reactive oxygen species (ROS) production, and coordinates their deployment by many interacting neutrophils. The potent inflammatory lipid mediator leukotriene B₄ (LTB₄) has been established as central to orchestrating neutrophil activities during swarming. However, the details regarding how this eicosanoid choreographs the neutrophils involved in swarming are not well explained. Here we leverage microfluidics, genetically deficient mouse cells, and targeted metabolipidomic analysis to demonstrate that transcellular biosynthesis occurs among neutrophils to generate LTB₄. Furthermore, transcellular biosynthesis is an entirely sufficient means of generating LTB₄ for the purposes of orchestrating neutrophil swarming. These results further our understanding of how neutrophils coordinate their activities during swarming, which will be critical in the design of eventual therapies that can harness the power of swarming behavior.

INTRODUCTION

Neutrophils have long been known for their critical role in the protection against fungal infections, featuring an armament of antimicrobial defenses (Desai and Lionakis, 2018). Among the most recently described is the behavior of swarming, during which neutrophils coordinate their own exponential recruitment to concentrate antimicrobial action against large targets (Kienle and Lämmermann, 2016). The role of LTB₄ as a critical mediator of neutrophil swarming has been well established in mice and humans by lipidomic analysis, antagonizing LTB₄ receptors, inhibiting LTB₄ biosynthesis, genetically manipulating intracellular LTB₄ signaling, and disrupting LTB₄ biosynthesis pathways (Hopke et al., 2020; Lämmermann et al., 2013; Malawista et al., 2008; Reategui et al., 2017). Despite these advances, details of LTB₄ biosynthesis and transport by neutrophils while swarming remain largely unexplored. A hint to potential complexity is provided by earlier studies showing that during inflammation, neutrophils exchange significant quantities of eicosanoid intermediates with other immune and non-immune cells (Serhan et al., 1984a, 2020). Transcellular eicosanoid biosynthesis adds flexibility and robustness to coordinate responses resulting from interactions between neutrophils and platelets (Hopke et al., 2020; Kienle et al., 2021; Lämmermann et al., 2013; Reategui et al., 2017), neutrophils and red blood cells (Stern and Serhan, 1989), neutrophils and endothelial cells (Claesson and Haeggstrom, 1988), neutrophils and airway epithelial cells, (Bigby et al., 1989) neutrophils and epidermal cells (Sola et al., 1992), neutrophils and lymphocytes (Odlander et al., 1988), etc. However, in this rich context, it is unknown if transcellular LTB₄ biosynthesis plays a role in coordinating neutrophil-neutrophil interactions during swarming. Here, we employ microfluidics, genetically deficient mouse cells, and targeted metabolipidomic analysis to probe the role of transcellular biosynthesis of LTB₄ during neutrophil swarming and restriction of pathogen growth.

RESULTS

We tested the ability of LTB₄ to restore the functions of neutrophils from mice with knockout genotypes at two critical steps in the LTB₄ synthesis pathway: 5-lipoxygenase (5-LOX) and leukotriene A₄ hydrolase (LTA₄H), encoded by *alox5* and *lta4h*, respectively (Wan et al., 2017). We verified that there were no significant differences in expression of the primary LTB₄ receptor BLT1 (Figure S1A) and no differences in chemotaxis toward LTB₄ (Figure 1A) between knockout and wild-type cell counterparts (C57/BL6 vs.

¹Center for Engineering in Medicine and Surgery, Massachusetts General Hospital, Boston, MA 02129, USA

²Harvard Medical School, Boston, MA 02115, USA

³Shriners Hospital for Children, Boston, MA 02114, USA

⁴Mucosal Immunology and Biology Research Center, Massachusetts General Hospital, Boston, MA 02114, USA

⁵Division of Infectious Diseases, Massachusetts General Hospital, Boston, MA 02114, USA

⁶Center for Experimental Therapeutics and Reperfusion Injury, Department of Anesthesiology, Perioperative, and Pain Medicine, Brigham and Women's Hospital and Harvard Medical School, Boston, MA 02115, USA

⁷These authors contributed equally

⁸Lead contact

*Correspondence: dirimia@mgh.harvard.edu (D.I.), bphurley@mgh.harvard.edu (B.P.H.)

<https://doi.org/10.1016/j.isci.2022.105226>



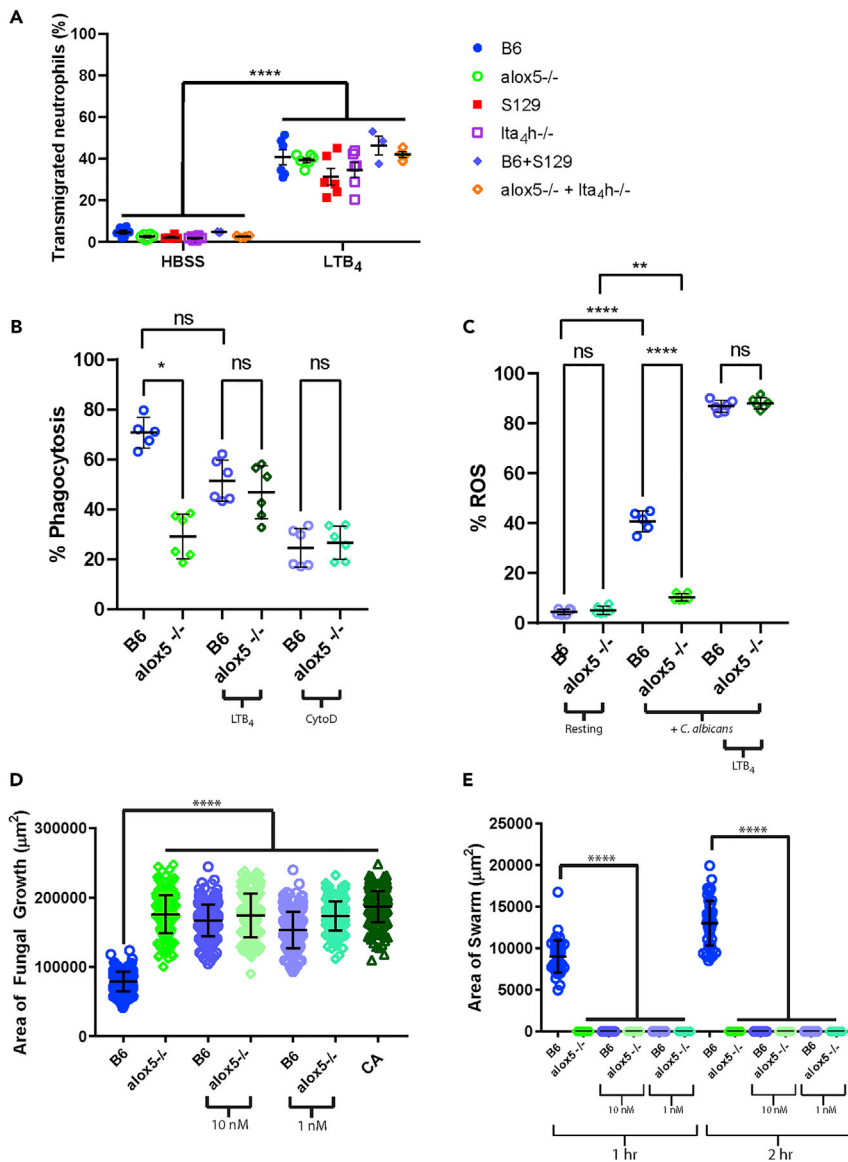


Figure 1. Neutrophil swarming is absent and cannot be restored by LTB₄ in neutrophils from alox5^{-/-} and Ita₄h^{-/-} mice, whereas common neutrophil functions are comparable to wild-type or could be restored by LTB₄

(A) Transmigration toward LTB₄ (0.2 ng/mL) through a membrane with 3 μm pores is comparable for bone marrow cells from B6 (C57/BL6 mice, the wild-type control for the alox5^{-/-} mice) and alox5^{-/-} or S129 (129S1/SvImJ mice, the wildtype control for the Ita₄h^{-/-} mice) and Ita₄h^{-/-} mice. There are no significant differences within the HBSS or the LTB₄ groups.

(B and C) The ability to phagocytose (B) *C. albicans* and produce ROS (C) by enriched neutrophils from alox5^{-/-} mice is restored by LTB₄ (0.6 nM) to levels comparable to C57 mice. N = 6 mice per genotype across 2 independent experiments. Phagocytosis events were differentiated from cell surface adherence events with the cytoskeletal inhibitor cytochalasin D (CytoD) at a concentration of 30 μM .

(D and E) Neutrophils enriched from the bone marrow of B6 and alox5^{-/-} mice, 500,000 neutrophils per genotype. Concentrations of 10 nM or 1 nM refer to LTB₄.

(D) The amount of fungal growth of *C. albicans* was quantified at 16 h after the start of the assay. CA refers to Candida alone, a condition in which only media is added to live *Candida albicans* targets. N \geq 282 swarms across three independent experiments.

(E) The area covered by the neutrophil swarm was quantified at the indicated timepoint. N = 48 swarms across 3 independent experiments. Mean and SD are shown, except for A, which is SEM ****p \leq 0.0001 by Kruskal-Wallis or one way ANOVA. See also Figure S1.

alox5^{-/-} and S129 vs. *Ita4h^{-/-}*). Consistent with the essential roles of LTB₄ in stimulating neutrophil phagocytosis and ROS production, we found significant differences in phagocytosis and ROS production between knockout and wild-type cells. These differences were corrected by the addition of exogenous LTB₄ (Figures 1B, 1C and S1B).

Next, we tested the swarming of mouse neutrophils triggered by 100 μm diameter clusters of live *Candida albicans*, a common example of an opportunistic fungal pathogen. We found swarming against these clusters as well as restriction of their growth to be completely defective in *alox5^{-/-}* cells, and these functions were not restored by the addition of LTB₄ (Figures 1D and 1E). In addition, the application of exogenous LTB₄ appeared to disrupt the ability of wild-type cells to swarm effectively and restrict fungal growth (Figures 1D and 1E). This result was surprising as it was established earlier that the process of swarming is LTB₄-signaling dependent (Hopke et al., 2020; Kienle et al., 2021; Lammermann et al., 2013; Malawista et al., 2008; Reategui et al., 2017). Our results confirm a critical role for LTB₄ signaling, as blocking of the primary LTB₄ receptor BLT1 disrupts swarming and restriction of *C. albicans* growth (Figures S2A and S2B). Of interest, LTB₄ levels appeared higher in the anti-BLT1 treated condition (Figure S2C). This may be due to an inability of the BLT1 receptor to bind and remove LTB₄ from the media. Despite this increased LTB₄, swarming is completely compromised, demonstrating the importance of sensing LTB₄ to an effective swarm response. Together, these results highlight the unique requirements for LTB₄ during swarming. These requirements depend not only on the presence of LTB₄ as observed with chemotaxis, phagocytosis, and ROS production, but also on context.

Further investigation of the relationship between LTB₄ and neutrophil swarming revealed that mixing the bone marrow cells derived from *alox5^{-/-}* and *Ita4h^{-/-}* mice in a 1:1 ratio restores their capacity to swarm (Figures 2A and 2B). This finding stands in stark contrast to their failure to swarm or restrict fungal growth when in genetically homogeneous populations (Figures 2 and S2D–S2F). The restoration is significant, with the ability of the mixed population of knockout neutrophils to restrict fungal growth comparable to that of their wild-type counterparts (Figure 2C). Full restoration in swarming is also observed when cells from knockout mice were mixed 1:1 with their appropriate wild-type counterparts (Figures S2D–S2F). These results suggest that, when mixed, cells with defects at different steps along the LTB₄ biosynthesis pathway can collaborate and compensate for their defects to restore their capacity to swarm and restrict fungal growth. We confirmed this finding using an enriched population of neutrophils (Figure S3), which matched those results obtained with bone marrow cells (Figure 2).

We hypothesized that the restoration of swarming in mixed knockout conditions might be due to transcellular biosynthesis of LTB₄ (Figure 3A). According to this hypothesis, the *Ita4h^{-/-}* neutrophils synthesize LTA₄ and share this precursor with neighboring cells, of which the *alox5^{-/-}* could complete the synthesis and the release of the LTB₄, which helps coordinate the activities of all mutant neutrophils possessing the BLT1 receptor. To directly test this hypothesis, we blocked LTB₄ signaling using an antagonist of BLT1. In agreement with our previous results (Figure S2), disruption of the LTB₄ signaling blocked swarming and reduced fungal restriction for the mixed wild-type cells (Figures 3B and 3C). Critically, blocking BLT1 signaling also disrupted swarming and fungal restriction for mixed knockout cells (Figures 3B and 3C). This result demonstrates that the restored ability of the mixed knockout cells to swarm is dependent on LTB₄ signaling, suggesting that transcellular LTB₄ biosynthesis is likely to occur when the knockout cells are mixed.

We measured LTB₄ release during swarming by ELISA and found that the mixed combination of *alox5^{-/-}* and *Ita4h^{-/-}* cells did release LTB₄, consistent with an occurrence of transcellular synthesis (Figure S4A). The amount of LTB₄ recovered from the mixed knockout population was less than that of LTB₄ recovered from the mixed combination of their respective wild-type cells. However, the magnitude of the swarming responses and the ability to restrict fungal growth is effectively the same as wild-type levels (Figures 3B and 3C). These results suggest that the generation of LTB₄ exclusively through transcellular biosynthesis of LTB₄ is sufficient to drive robust swarming responses even though the amount of LTB₄ generated appears to be less (Figures 2, 3 and S4A).

Paradoxically, a homogeneous population of *Ita4h^{-/-}* cells appears to be producing low levels of LTB₄ as measured by ELISA, despite lacking a critical biosynthetic enzyme for this process (Figure S4A). This observation was confirmed by ELISA with LTB₄ assayed from supernatant following stimulation with calcium

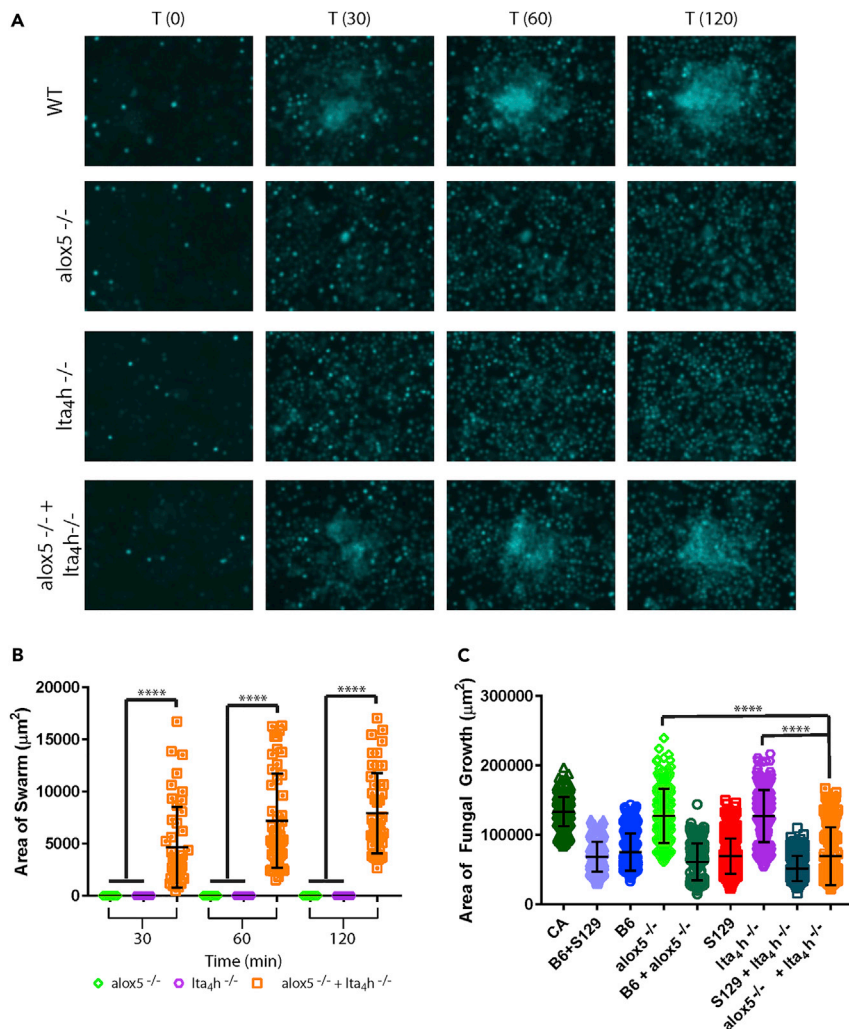


Figure 2. Swarming responses against *C. albicans* are absent in homogeneous and restored in heterogeneous populations of bone marrow cells

(A) Fluorescence imaging (Hoechst) of mouse bone marrow cells swarming against live *C. albicans* target. 500,000 bone marrow cells from wild-type, alox5^{-/-}, lta4h^{-/-}, and equal numbers of alox5^{-/-} + lta4h^{-/-} mice were added to swarming arrays. Representative images of swarming from wild-type cells, alox5^{-/-} or lta4h^{-/-} cells alone and alox5^{-/-} + lta4h^{-/-} mixed together 1:1 are shown. T is in minutes.

(B) The size of the neutrophil swarms formed against *C. albicans* targets was quantified over time. N = 48 swarms across 3 independent experiments.

(C) The amount of fungal growth of *C. albicans* was quantified 16 h after the start of the assay. N ≥ 254 targets across three independent experiments. Mean and SD are shown. ****p < 0.0001 by Kruskal-Wallis post-test. See also Figures S2 and S3.

ionophore in the absence of *C. albicans*, suggesting that the presence of fungi and the possibility of a fungal source of LTA₄H is not an explanation for the ELISA signal associated with lta4h^{-/-} neutrophils (Figure S4B). To better resolve whether this ELISA signal from lta4h^{-/-} neutrophils is real, given its low level, the supernatant was also collected using an enriched population of neutrophils responding to live *C. albicans*, which once more confirmed the presence of this ELISA signal associated with lta4h^{-/-} neutrophils (Figure S4C). One potential explanation for why lta4h^{-/-} neutrophils generated a positive LTB₄ ELISA signal is because, unlike alox5^{-/-} cells, lta4h^{-/-} cells remain capable of producing leukotriene A₄ (LTA₄). In the absence of LTA₄H, LTA₄ is rapidly converted non-enzymatically to inactive breakdown metabolites, including 6-trans-LTB₄ (Haeggstrom, 2018). It is possible that LTA₄ and breakdown metabolites are indistinguishable from LTB₄ in this ELISA, and supernatant from lta4h^{-/-} neutrophils that produce LTA₄ breakdown products yield a positive signal despite not containing any actual LTB₄. In support of this

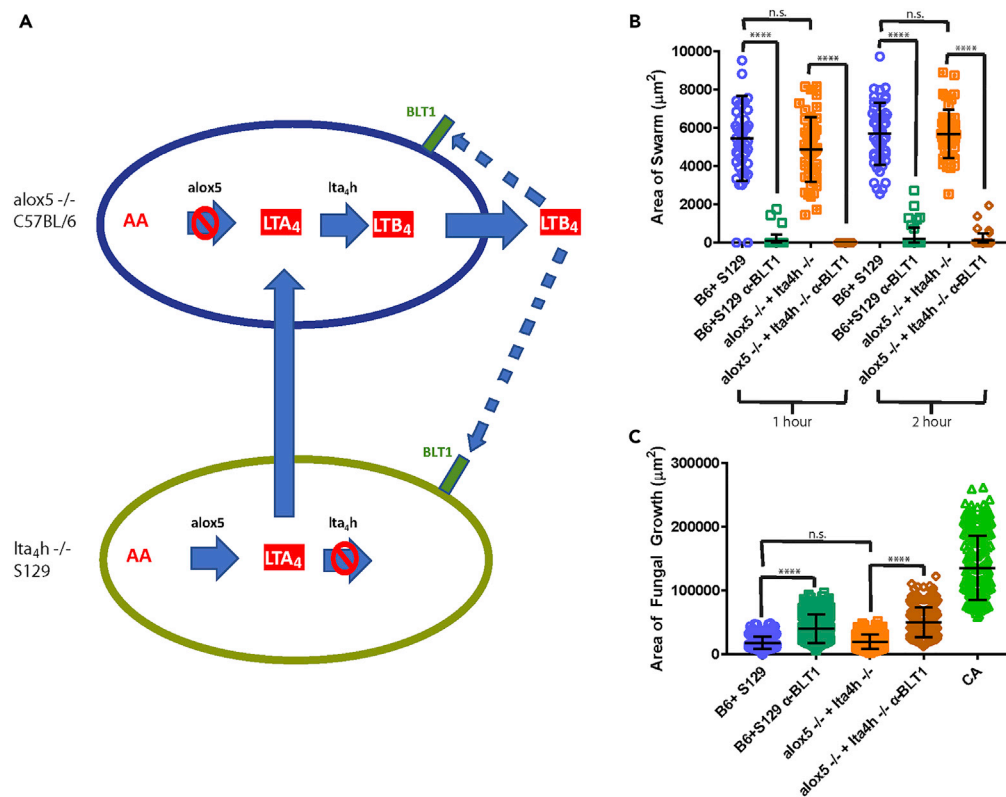


Figure 3. Transcellular synthesis is sufficient to restore swarming responses against *C. albicans*

(A) A schematic diagram indicates the important steps in LTB₄ synthesis, the block points for *alox5*^{-/-} and *Ita4h*^{-/-} cell types, how they can collaborate by transcellular synthesis to create LTB₄, and how LTB₄ signals through BLT1 receptors present on both cell types to drive swarming.

(B) Bone marrow cells of the indicated genotypes were pre-incubated with 10 μM of the BLT1 antagonist U-75302 or vehicle for 30 min and then added to the swarming assay. The area of the swarm was quantified at 1 and 2 h. N = 48 swarms across three independent experiments.

(C) The area of fungal growth at the end of the assay (16 h) was also quantified. N ≥ 286 swarms across three independent experiments. Mean and SD are shown. n.s. is non-significant and ****p ≤ 0.0001 by Kruskal-Wallis with Dunn's post-test. See also Figure S2.

interpretation, a bioactivity assay that takes advantage of the chemotactic potential of LTB₄ (not shared by LTA₄ breakdown metabolites) was developed and revealed that the supernatant from swarming chambers containing either *alox5*^{-/-} or *Ita4h*^{-/-} neutrophils alone failed to elicit a response, consistent with a lack of true LTB₄ production for *Ita4h*^{-/-} neutrophils (Figure S4D). A significant increase in directed migration of neutrophils across a permeable Transwell was observed when supernatant was derived from a 1:1 mix of *alox5*^{-/-} and *Ita4h*^{-/-}, thereby revealing the presence of chemotactic bioactivity that was exclusively associated with the mixture of *alox5*^{-/-} and *Ita4h*^{-/-} cells and this bioactivity likely represents LTB₄ generated by transcellular means (Figure S4D).

To further confirm that transcellular biosynthesis of LTB₄ is occurring when mixing *alox5*^{-/-} and *Ita4h*^{-/-} cells and to unambiguously clarify the nature of molecules detected by the ELISA, we conducted mass spectrometry on collected supernatants (Figure 4A and Table 1). Bone marrow cells derived from *alox5*^{-/-} mice failed to generate LTB₄ and produced trace amounts of LTA₄ non-enzymatic breakdown metabolites (Figures 4B, 4C and Table 1). Cells from *Ita4h*^{-/-} mice also failed to generate LTB₄ but did produce significant LTA₄ and breakdown metabolites, 6-trans-LTB₄, 6-trans-12-*epi*-LTB₄, 5S,6S-diHETE, 5S,6R-diHETE as anticipated (Figures 4B, 4C and Table 1). The mixture of the *alox5*^{-/-} and *Ita4h*^{-/-} cells resulted in the biosynthesis of LTB₄ through transcellular processes as individual knockout neutrophils in isolation are incapable of generating LTB₄ (Figures 4B, 4C and Table 1). In agreement with our ELISA results (Figure S4A), the amount of LTB₄ produced in this condition of exclusively transcellular biosynthesis

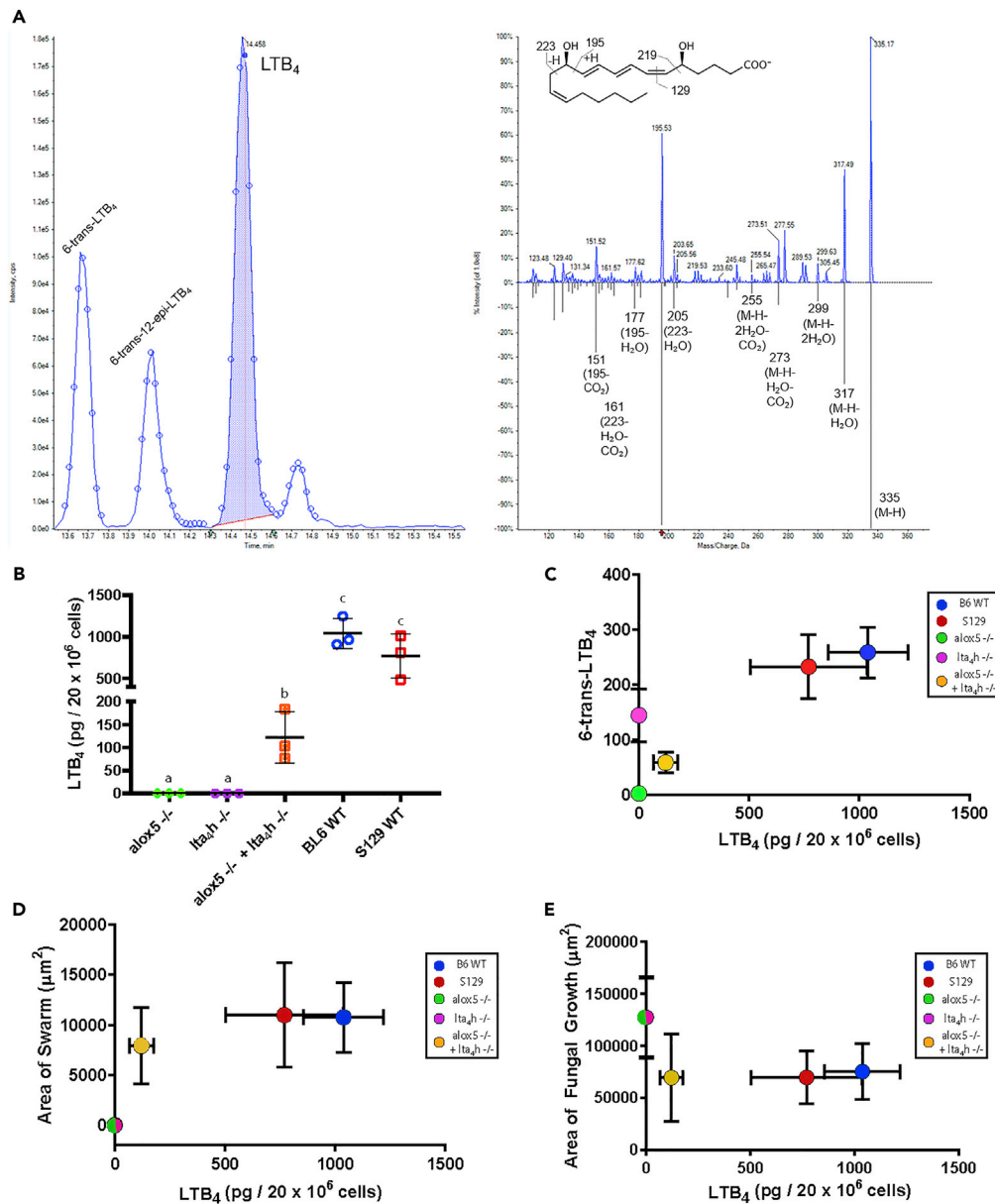


Figure 4. Heterogeneous mixtures of *alox5*^{-/-} and *Ita4h*^{-/-} biosynthesize leukotriene B₄

(A) LC-MS/MS targeted multiple reaction monitoring for *m/z* 335>195. The green arrows indicate the time interval of the quantitation (shaded). The selected data point denotes the time and intensity at which the spectrum, shown on the right, was recorded. Right, Enhanced product ion spectra of LTB₄, top spectrum is from bone marrow cells, and the bottom spectrum is from the custom metabololipidomics library. The red arrow indicates Q3 (*m/z* 195). Inset, LTB₄ structure with fragmentation. LTB₄ fit from samples to LTB₄ in custom metabololipidomics library (99.4%, see STAR Methods).

(B) The amount of LTB₄ detected in each condition was quantified. N= three independent experiments per group.

(C–E) Dots represent the average of the indicated conditions, with error bars representing SD.

(C) The amount of LTB₄ is compared to the amount of 6-trans-LTB₄ detected in each group.

(D) The average area of a neutrophil swarm for each condition at 2 h was plotted against the amount of LTB₄ detected in the group.

(E) The average area of fungal growth at 16 h for each condition was plotted against the amount of LTB₄ detected in the group. Unshared letters represent significant differences between groups. *p* ≤ 0.05 by Student's unpaired two-tailed *t*-test. See also Figures S3 and S4.

Table 1. Quantification of lipid mediators released during swarming

	LTB ₄	6-trans-LTB ₄	6-trans-12-epi-LTB ₄	5S,6S-diHETE	5S,6R-diHETE
<i>alox5</i> ^{-/-}	0.0	2 ± 0.4	4 ± 0.6	0.0	0.0
<i>lta4h</i> ^{-/-}	0.0	144 ± 48	181 ± 62	50 ± 24	17 ± 20
<i>alox5</i> ^{-/-} + <i>lta4h</i> ^{-/-}	121 ± 55	58 ± 19	41 ± 14	11 ± 4	7 ± 3
BL6 WT	1039 ± 181	258 ± 46	73 ± 3	27 ± 2	22 ± 1
S129 WT	770 ± 265	232 ± 58	81 ± 28	29 ± 9	19 ± 7
Media	0.0	0.0	0.0	0.0	0.0

Twenty million bone marrow cells from mice of the indicated genotypes were harvested and added to large swarming arrays of *C. albicans*. Supernatants and cells were harvested after 2 h and subjected to LC-MS/MS to examine lipid mediator biosynthesis. Concentrations represent picogram per 2×10^7 cells and are the average \pm SD of three independent experiments.

(*alox5*^{-/-} + *lta4h*^{-/-} neutrophils) is significantly lower than that produced during swarming by either wild-type cells (Figures 4B and 4C). Importantly, despite the difference in the magnitude of LTB₄ biosynthesized, both swarming and fungal control are preserved and comparable between the mixed knockout and mixed wild-type counterpart conditions (Figures 3B, 3C, 4D and 4E).

DISCUSSION

We measured mouse neutrophil swarming against *C. albicans* cluster targets and found that transcellular biosynthesis of LTB₄ drives swarming responses that restrict the growth of fungi. Interfering with the LTB₄ biosynthesis through deletion of key synthetic enzymes in *alox5*^{-/-} and *lta4h*^{-/-} mouse neutrophils and antagonizing LTB₄ receptors disrupts swarming. Notably, the swarming of *alox5*^{-/-} mouse neutrophils cannot be restored by the addition of LTB₄. These results reveal an essential role for the coordinated LTB₄ release from neutrophils in accomplishing the swarming choreography. The dependence on coordinated LTB₄ release distinguishes swarming from other 'traditional' neutrophil functions. For example, phagocytosis and ROS production are also altered when LTB₄ biosynthesis is prevented in *alox5*^{-/-} mouse neutrophils, but, unlike swarming, phagocytosis and ROS production in these cells are restored by exposing the neutrophils to extrinsic LTB₄, consistent with the previous reports (Miralda et al., 2017). Our study shows that swarming can only be restored when mixing *alox5*^{-/-} and *lta4h*^{-/-} neutrophils, where transcellular biosynthesis of LTB₄ becomes possible. Furthermore, antagonizing LTB₄ receptors disrupts swarming in these mixed cell experiments. These results highlight swarming as a unique and higher-order function of neutrophil coordination, which is more than simply the sum of activities manifested by individually functioning neutrophils.

Swarming, as an emergent neutrophil behavior, has been recently visualized in the context of mechanical (Alexander et al., 2020; Barros et al., 2021; Hopke et al., 2020; Knooihuizen et al., 2021; Yonker et al., 2021), thermal (Lammermann et al., 2013), or infected wounds (Chtanova et al., 2008) in mice and zebrafish. For human neutrophils, ex vivo testing revealed disrupted swarming in patient populations at risk for fungal infections, e.g., transplant recipients, cirrhosis, trauma, chronic granulomatous disease, cystic fibrosis, etc. (Barros et al., 2021; Hopke et al., 2020; Knooihuizen et al., 2021; Yonker et al., 2021). Furthermore, in a single patient case study, we found that restoring neutrophil swarming correlated with reduced numbers of infections experienced by that patient (Alexander et al., 2020). In parallel efforts, lipid mediators are increasingly understood to be consequential in various pathological processes, and targeting biosynthesis may have therapeutic benefits in these circumstances (Haeggstrom, 2018). The range of conditions that could be corrected by the manipulation of lipid mediator levels spans from common infections (Jordan and Werz, 2021) to complex conditions like Alzheimer's disease (Emre et al., 2022).

Our understanding of transcellular biosynthesis of lipid mediators in homogeneous cell populations benefits from earlier studies in heterogeneous mixtures of neutrophils with other cell types (Fabre et al., 2002). Transcellular biosynthesis helps coordinate the activity of immune and non-immune cells sharing the same space, e.g., neutrophils, lymphocytes, platelets, and endothelial cells (Claesson and Haeggstrom, 1988; Fiore and Serhan, 1990; Marcus et al., 1982; Odlander et al., 1988; Serhan et al., 1984a, 1984b, 2020). Transcellular biosynthesis is facilitated by the proximity of two distinct cell types that individually lack but collectively express all necessary enzymes to synthesize a particular mediator (Corey et al., 1980). One of the eicosanoid intermediates that is most shared among immune and non-immune cells is LTA₄, produced

and released in large amounts by neutrophils (Afonso et al., 2012; Fiore and Serhan, 1989). When LTA₄ is taken up by endothelial cells, keratinocytes, erythrocytes, or alveolar macrophages, which express LTA₄ hydrolase, these cells can biosynthesize LTB₄ (Dieterle et al., 2020). An indication that transcellular biosynthesis is likely to be quite common is the observation that close to half of the LTA₄ produced by neutrophils is released extracellularly rather than converted to LTB₄ (Claesson and Haeggstrom, 1988; Fiore and Serhan, 1990; Marcus et al., 1982; Odlander et al., 1988; Serhan et al., 1984a, 1984b, 2020).

Our study raises several important questions that will be addressed in future studies. It is not fully understood how transcellular biosynthesis intermediates are transported between neutrophils. For transcellular biosynthesis of LTB₄ to occur, LTA₄ must be passed from *Ita4h*^{-/-} neutrophils, which have functional 5-LOX, to the *alox5*^{-/-} neutrophils, which have functional LTA₄ hydrolase. By collaborating in this fashion, the *alox5*^{-/-} and *Ita4h*^{-/-} cells can produce functional LTB₄, which can then be released to drive the recruitment and swarming of both cell types. LTA₄ has a short half-life (Fiore and Serhan, 1989; Haeggstrom, 2018; Stsiapanava et al., 2017) and is likely hydrolyzed immediately after release (Fiore and Serhan, 1989). Transportation modes that increase the biological half-life of LTA₄ should be considered. For example, associations of LTA₄ to lipid membranes (Fiore and Serhan, 1989) and to chaperone molecules, like albumin (Fitzpatrick et al., 1982), have been proposed to protect LTA₄ in the extracellular space between various cell pairs. A transport mediated by exosomes has also been suggested for shuttling LTB₄ from neutrophils to other neutrophils (Dieterle et al., 2020) and may also be applicable to LTA₄. This mechanism may also be consistent with the relay model of neutrophil signaling during swarming (Dieterle et al., 2020).

Limitations of the study

Much of this work was conducted with bone marrow cells that feature 40% or less mature neutrophils within the total cell population. It is, therefore, possible that other cells within the bone marrow may influence the swarming observed herein. Our observations were confirmed using enriched neutrophil populations (65–75% mature neutrophils) from bone marrow. Nevertheless, further work is needed to exclude potential influences of the non-neutrophil cellular component within the bone marrow.

The relevance of our findings in mice to human neutrophils remains to be examined. Human neutrophils display multiple levels of redundancy in swarming, with additional factors besides LTB₄, like IL-8 and complement factors, partially compensating for the loss of LTB₄. Unlike human neutrophils, LTB₄ appears to be the only driving factor of neutrophil swarming in mice (Hopke et al., 2020; Kienle et al., 2021; Lammermann et al., 2013; Reategui et al., 2017). Our study demonstrates that transcellular LTB₄ biosynthesis is necessary and sufficient to orchestrate swarming and restriction of fungal growth by a mixture of genetically deficient mouse neutrophils that are individually incapable of completing LTB₄ synthesis. We suggest that transcellular LTB₄ biosynthesis is likely to be important in orchestrating wild-type mouse neutrophil swarming as well. Transcellular LTB₄ biosynthesis is facilitated by the large proportion of LTA₄ released from wild-type neutrophils as revealed by detection of LTA₄ non-enzymatic breakdown metabolites (Afonso et al., 2012; Fiore and Serhan, 1989). Future investigations are necessary to characterize the role of LTB₄ transcellular biosynthesis in human and mouse swarming and its contribution to neutrophil-mediated host defense following sterile injury and infection.

STAR★METHODS

Detailed methods are provided in the online version of this paper and include the following:

- KEY RESOURCES TABLE
- RESOURCE AVAILABILITY
 - Lead contact
 - Materials availability
 - Data and code availability
- EXPERIMENTAL MODEL AND SUBJECT DETAILS
 - Animals
 - Microbial strains
- METHOD DETAILS
 - Isolation of bone marrow cells and purification of bone marrow neutrophils
 - Phagocytosis and ROS production during *C. albicans* challenge

- Swarming array printing
- Patterning of *Candida albicans* cluster targets
- Swarming experiments
- Image analysis
- Bone marrow cell culture
- LTB₄ quantification by ELISA
- BLT1 receptor quantification on mouse neutrophils
- Chemotaxis assay
- Targeted liquid chromatography-tandem mass spectrometry metabololipidomics
- **QUANTIFICATION AND STATISTICAL ANALYSIS**

SUPPLEMENTAL INFORMATION

Supplemental information can be found online at <https://doi.org/10.1016/j.isci.2022.105226>.

ACKNOWLEDGMENTS

We acknowledge funding from the National Institutes of Health (GM092804 to DI, AI095338 to BPH, AI132638 to MKM, GM095467 & GM139430 to CNS), and from the Shriners Hospitals for Children (71010-BOS-22 to DI). Graphical Abstract illustrated by Nicole Wolf, MS, ©2022 (nicolecwoolf@gmail.com).

AUTHOR CONTRIBUTIONS

Conceptualization: A.R.H., T.L., D.I., B.P.H.; Investigation: A.R.H., T.L., A.K.S., A.E.S., K.D.T., B.W.M., and M.K.M.; Writing – Original Draft: A.R.H., D.I., and B.P.H.; Writing – Review and Editing, A.R.H., T.L., A.K.S., A.E.S., K.D.T., B.W.M., M.K.M., C.N.S., D.I., B.P.H.; Supervision: M.K.M., C.N.S., D.I., and B.P.H.; Funding Acquisition: D.I. and B.P.H.

DECLARATION OF INTERESTS

M.K.M. reports consultation fees from Vericel, Pulsethera, NED Biosystems, GenMark Diagnostics, Clear Creek Bio, and Day Zero Diagnostics; grant support from Thermo Fisher Scientific and Genentech; medical editing/writing fees from UpToDate, outside the submitted work. M.K.M. also reports patents 14/110,443 and 15/999,463 pending.

Received: April 28, 2022

Revised: July 25, 2022

Accepted: September 23, 2022

Published: October 21, 2022

REFERENCES

- Afonso, P.V., Janka-Junttila, M., Lee, Y.J., McCann, C.P., Oliver, C.M., Aamer, K.A., Losert, W., Cicerone, M.T., and Parent, C.A. (2012). LTB₄ is a signal-relay molecule during neutrophil chemotaxis. *Dev. Cell* 22, 1079–1091. <https://doi.org/10.1016/j.devcel.2012.02.003>.
- Alexander, N.J., Bozym, D.J., Farmer, J.R., Parris, P., Viens, A., Atallah, N., Hopke, A., Scherer, A., Dagher, Z., Barros, N., et al. (2020). Neutrophil functional profiling and cytokine augmentation for patients with multiple recurrent infections: a case study. *J. Allergy Clin. Immunol. Pract.* 9, 986–988. <https://doi.org/10.1016/j.jaip.2020.08.024>.
- Barros, N., Alexander, N., Viens, A., Timmer, K., Atallah, N., Knooihuizen, S.A.I., Hopke, A., Scherer, A., Dagher, Z., Irimia, D., and Mansour, M.K. (2021). Cytokine augmentation reverses transplant recipient neutrophil dysfunction against the human fungal pathogen, *Candida albicans*. *J. Infect. Dis.* 224, 894–902. <https://doi.org/10.1093/infdis/jiab009>.
- Bigby, T.D., Lee, D.M., Meslier, N., and Gruenert, D.C. (1989). Leukotriene A₄ hydrolase activity of human airway epithelial cells. *Biochem. Biophys. Res. Commun.* 164, 1–7. [https://doi.org/10.1016/0006-291x\(89\)91674-4](https://doi.org/10.1016/0006-291x(89)91674-4).
- Boxio, R., Bossenmeyer-Pourié, C., Steinckwich, N., Dournon, C., and Nüsse, O. (2004). Mouse bone marrow contains large numbers of functionally competent neutrophils. *J. Leukoc. Biol.* 75, 604–611. <https://doi.org/10.1189/jlb.0703340>.
- Byrum, R.S., Goulet, J.L., Snouwaert, J.N., Griffiths, R.J., and Koller, B.H. (1999). Determination of the contribution of cysteinyl leukotrienes and leukotriene B₄ in acute inflammatory responses using 5-lipoxygenase- and leukotriene A₄ hydrolase-deficient mice. *J. Immunol.* 163, 6810–6819.
- Chen, X.S., Sheller, J.R., Johnson, E.N., and Funk, C.D. (1994). Role of leukotrienes revealed by targeted disruption of the 5-lipoxygenase gene. *Nature* 372, 179–182. <https://doi.org/10.1038/372179a0>.
- Chtanova, T., Schaeffer, M., Han, S.J., van Dooren, G.G., Nollmann, M., Herzmark, P., Chan, S.W., Satija, H., Camfield, K., Aaron, H., et al. (2008). Dynamics of neutrophil migration in lymph nodes during infection. *Immunity* 29, 487–496. <https://doi.org/10.1016/j.immuni.2008.07.012>.
- Claesson, H.E., and Haeggstrom, J. (1988). Human endothelial cells stimulate leukotriene synthesis and convert granulocyte released leukotriene A₄ into leukotrienes B₄, C₄, D₄ and E₄. *Eur. J. Biochem.* 173, 93–100. <https://doi.org/10.1111/j.1432-1033.1988.tb13971.x>.
- Corey, E.J., Marfat, A., Goto, G., and Brion, F. (1980). Leukotriene B. Total synthesis and assignment of stereochemistry. *J. Am. Chem. Soc.* 102, 7984–7985. <https://doi.org/10.1021/ja00547a051>.
- Desai, J.V., and Lionakis, M.S. (2018). The role of neutrophils in host defense against invasive

- fungal infections. *Curr. Clin. Microbiol. Rep.* 5, 181–189. <https://doi.org/10.1007/s40588-018-0098-6>.
- Dieterle, P.B., Min, J., Irimia, D., and Amir, A. (2020). Dynamics of diffusive cell signaling relays. *Elife* 9, e61771. <https://doi.org/10.7554/eLife.61771>.
- Emre, C., Arroyo-García, L.E., Do, K.V., Jun, B., Ohshima, M., Alcalde, S.G., Cothorn, M.L., Maioli, S., Nilsson, P., Hjorth, E., et al. (2022). Intranasal delivery of pro-resolving lipid mediators rescues memory and gamma oscillation impairment in App(NL-G-F/NL-G-F) mice. *Commun. Biol.* 5, 245. <https://doi.org/10.1038/s42003-022-03169-3>.
- Fabre, J.E., Goulet, J.L., Riche, E., Nguyen, M., Coggins, K., Offenbacher, S., and Koller, B.H. (2002). Transcellular biosynthesis contributes to the production of leukotrienes during inflammatory responses in vivo. *J. Clin. Invest.* 109, 1373–1380. <https://doi.org/10.1172/JCI14869>.
- Fiore, S., and Serhan, C.N. (1989). Phospholipid bilayers enhance the stability of leukotriene A4 and epoxytetraenes: stabilization of eicosanoids by liposomes. *Biochem. Biophys. Res. Commun.* 159, 477–481. [https://doi.org/10.1016/0006-291x\(89\)90017-x](https://doi.org/10.1016/0006-291x(89)90017-x).
- Fiore, S., and Serhan, C.N. (1990). Formation of lipoxins and leukotrienes during receptor-mediated interactions of human platelets and recombinant human granulocyte/macrophage colony-stimulating factor-primed neutrophils. *J. Exp. Med.* 172, 1451–1457. <https://doi.org/10.1084/jem.172.5.1451>.
- Fitzpatrick, F.A., Morton, D.R., and Wynalda, M.A. (1982). Albumin stabilizes leukotriene A4. *J. Biol. Chem.* 257, 4680–4683.
- Haeggstrom, J.Z. (2018). Leukotriene biosynthetic enzymes as therapeutic targets. *J. Clin. Invest.* 128, 2680–2690. <https://doi.org/10.1172/JCI97945>.
- Hopke, A., Nicke, N., Hidu, E.E., Degani, G., Popolo, L., and Wheeler, R.T. (2016). Neutrophil attack triggers extracellular trap-dependent *Candida* cell wall remodeling and altered immune recognition. *PLoS Pathog.* 12, e1005644. <https://doi.org/10.1371/journal.ppat.1005644>.
- Hopke, A., Scherer, A., Kreuzburg, S., Abers, M.S., Zerbe, C.S., Dinauer, M.C., Mansour, M.K., and Irimia, D. (2020). Neutrophil swarming delays the growth of clusters of pathogenic fungi. *Nat. Commun.* 11, 2031. <https://doi.org/10.1038/s41467-020-15834-4>.
- Hurley, B.P., Siccardi, D., Mrsny, R.J., and McCormick, B.A. (2004). Polymorphonuclear cell transmigration induced by *Pseudomonas aeruginosa* requires the eicosanoid hepxilin A3. *J. Immunol.* 173, 5712–5720. <https://doi.org/10.4049/jimmunol.173.9.5712>.
- Jordan, P.M., and Werz, O. (2021). Specialized pro-resolving mediators: biosynthesis and biological role in bacterial infections. *FEBS J.* 289, 4212–4227. <https://doi.org/10.1111/febs.16266>.
- Kienle, K., Glaser, K.M., Eickhoff, S., Mihlan, M., Knöpper, K., Reátegui, E., Epple, M.W., Gunzer, M., Baumeister, R., Tarrant, T.K., et al. (2021). Neutrophils self-limit swarming to contain bacterial growth in vivo. *Science* 372, eabe7729. <https://doi.org/10.1126/science.abe7729>.
- Kienle, K., and Lämmermann, T. (2016). Neutrophil swarming: an essential process of the neutrophil tissue response. *Immunol. Rev.* 273, 76–93. <https://doi.org/10.1111/imr.12458>.
- Knooihuizen, S.A.I., Alexander, N.J., Hopke, A., Barros, N., Viens, A., Scherer, A., Atallah, N.J., Dagher, Z., Irimia, D., Chung, R.T., and Mansour, M.K. (2021). Loss of coordinated neutrophil responses to the human fungal pathogen, *Candida albicans*, in patients with cirrhosis. *Hepatol. Commun.* 5, 502–515. <https://doi.org/10.1002/hep4.1645>.
- Lämmermann, T., Afonso, P.V., Angermann, B.R., Wang, J.M., Kastenmuller, W., Parent, C.A., and Germain, R.N. (2013). Neutrophil swarms require LTB4 and integrins at sites of cell death in vivo. *Nature* 498, 371–375. <https://doi.org/10.1038/nature12175>.
- Malawista, S.E., de Boisfleury Chevance, A., van Damme, J., and Serhan, C.N. (2008). Tonic inhibition of chemotaxis in human plasma. *Proc. Natl. Acad. Sci. USA* 105, 17949–17954. <https://doi.org/10.1073/pnas.0802572105>.
- Marcus, A.J., Broekman, M.J., Safier, L.B., Ullman, H.L., Islam, N., Sherhan, C.N., Rutherford, L.E., Korchak, H.M., and Weissmann, G. (1982). Formation of leukotrienes and other hydroxy acids during platelet-neutrophil interactions in vitro. *Biochem. Biophys. Res. Commun.* 109, 130–137. [https://doi.org/10.1016/0006-291x\(82\)91575-3](https://doi.org/10.1016/0006-291x(82)91575-3).
- McCormick, B.A., Hofman, P.M., Kim, J., Carnes, D.K., Miller, S.I., and Madara, J.L. (1995). Surface attachment of *Salmonella typhimurium* to intestinal epithelia imprints the subepithelial matrix with gradients chemotactic for neutrophils. *J. Cell Biol.* 131, 1599–1608. <https://doi.org/10.1083/jcb.131.6.1599>.
- Miralda, I., Uriarte, S.M., and McLeish, K.R. (2017). Multiple phenotypic changes define neutrophil priming. *Front. Cell. Infect. Microbiol.* 7, 217. <https://doi.org/10.3389/fcimb.2017.00217>.
- Odlander, B., Jakobsson, P.J., Rosén, A., and Claesson, H.E. (1988). Human B and T lymphocytes convert leukotriene A4 into leukotriene B4. *Biochem. Biophys. Res. Commun.* 153, 203–208. [https://doi.org/10.1016/s0006-291x\(88\)1209-9](https://doi.org/10.1016/s0006-291x(88)1209-9).
- Reategui, E., Jalali, F., Khankhel, A.H., Wong, E., Cho, H., Lee, J., Serhan, C.N., Dalli, J., Elliott, H., and Irimia, D. (2017). Microscale arrays for the profiling of start and stop signals coordinating human-neutrophil swarming. *Nat. Biomed. Eng.* 1, 0094. <https://doi.org/10.1038/s41551-017-0094>.
- Serhan, C.N., Gupta, S.K., Perretti, M., Godson, C., Brennan, E., Li, Y., Soehnlein, O., Shimizu, T., Werz, O., Chirchiu, V., et al. (2020). The atlas of inflammation resolution (AIR). *Mol. Aspects Med.* 74, 100894. <https://doi.org/10.1016/j.mam.2020.100894>.
- Serhan, C.N., Lundberg, U., Lindgren, J.A., Weissmann, G., and Samuelsson, B. (1984a). Formation of leukotriene C4 by human leukocytes exposed to monosodium urate crystals. *FEBS Lett.* 167, 109–112. [https://doi.org/10.1016/0014-5793\(84\)80842-x](https://doi.org/10.1016/0014-5793(84)80842-x).
- Serhan, C.N., Lundberg, U., Weissmann, G., and Samuelsson, B. (1984b). Formation of leukotrienes and hydroxy acids by human neutrophils and platelets exposed to monosodium urate. *Prostaglandins* 27, 563–581. [https://doi.org/10.1016/0090-6980\(84\)90092-3](https://doi.org/10.1016/0090-6980(84)90092-3).
- Shay, A.E., Nshimiyimana, R., Samuelsson, B., Petasis, N.A., Haeggström, J.Z., and Serhan, C.N. (2021). Human leukocytes selectively convert 4S, 5S-epoxy-resolvin to resolvin D3, resolvin D4, and a cys-resolvin isomer. *Proc. Natl. Acad. Sci. USA* 118, e2116559118. <https://doi.org/10.1073/pnas.2116559118>.
- Sola, J., Godessart, N., Vila, L., Puig, L., and de Moragas, J.M. (1992). Epidermal cell-polymorphonuclear leukocyte cooperation in the formation of leukotriene B4 by transcellular biosynthesis. *J. Invest. Dermatol.* 98, 333–339. <https://doi.org/10.1111/1523-1747.ep12499800>.
- Stern, A., and Serhan, C.N. (1989). Human red cells enhance the formation of 5-lipoxygenase-derived products by neutrophils. *Free Radic. Res. Commun.* 7, 335–339. <https://doi.org/10.3109/10715768909087959>.
- Stsiapanava, A., Samuelsson, B., and Haeggström, J.Z. (2017). Capturing LTA4 hydrolase in action: insights to the chemistry and dynamics of chemotactic LTB4 synthesis. *Proc. Natl. Acad. Sci. USA* 114, 9689–9694. <https://doi.org/10.1073/pnas.1710850114>.
- Wan, M., Tang, X., Stsiapanava, A., and Haeggström, J.Z. (2017). Biosynthesis of leukotriene B4. *Semin. Immunol.* 33, 3–15. <https://doi.org/10.1016/j.smim.2017.07.012>.
- Wang, G., Calvo, K., Pasillas, M. D.B., Sykes, H., and Häcker, M.P. (2006). Kamps Quantitative production of macrophages or neutrophils *in vivo* using conditional *Hoxb8*. *Nat. Methods* 3, 287–293. <https://doi.org/10.1038/nmeth865>.
- Yonker, L.M., Marand, A., Muldur, S., Hopke, A., Leung, H.M., De La Flor, D., Park, G., Pinsky, H., Guthrie, L.B., Tearney, G.J., et al. (2021). Neutrophil dysfunction in cystic fibrosis. *J. Cyst. Fibros.* 20, 1062–1071. <https://doi.org/10.1016/j.jcf.2021.01.012>.

STAR★METHODS

KEY RESOURCES TABLE

REAGENT or RESOURCE	SOURCE	IDENTIFIER
Antibodies		
Mouse monoclonal PE anti-human CD45	Biolegend	Cat#304058; RRID: AB_2564156
Mouse monoclonal PerCP-Cy5.5 anti-human CD16	Biolegend	Cat#302028; RRID: AB_893263
Mouse monoclonal APC anti-human CD66b	Invitrogen	Cat#17-0666-42; RRID: AB_2573152
Rabbit polyclonal Alexa fluor 488 anti-human BLT1	Bioss	Cat# bs-2654R-A488; RRID: AB_2924305
Mouse monoclonal anti-human CD16/32	Invitrogen	Cat#14-0161-82; RRID: AB_467133
PE anti-mouse Ly-6G Antibody, clone 1A8	BioLegend	Cat#127608; RRID: AB_1186099
Chemicals, peptides, and recombinant proteins		
U-75302	Cayman Chemicals	70705; CAS 119477-85-9
SYTOX Green	ThermoFisher Scientific	S7020
Leukotriene B ₄	Cayman Chemicals	20110;CAS 71160-24-2
Dihydrorhodamine 123	ThermoFisher Scientific	Cat#D23806
Cytochalasin D – from <i>Zygosporium mansonii</i>	Sigma-Aldrich	Cat#C8273
Poly-L-Lysine solution- 0.1% in H ₂ O	Sigma-Aldrich	P8920-100ML
d ₄ -Leukotriene B ₄	Cayman Chemicals	Cat#320110
Methanol, Optima LC/MS Grade	Thermo Fisher Scientific	Cat#A456-4
OmniSolv Hexanes 64% n-hexane For HPLC, Spectrophotometry and Gas Chromatography	VWR	Cat#HX0296P-1
Methyl Formate	Sigma-Aldrich	Cat#259705-2L
Water, Optima LC/MS Grade	Thermo Fisher Scientific	Cat#W6-4
Formic Acid (ACS Reagent, ≥ 96%)	Sigma-Aldrich	Cat#695076-500ML
6-trans-Leukotriene B ₄	Cayman Chemicals	Cat#35250
6-trans-12-epi-Leukotriene B ₄	Cayman Chemicals	Cat#35265
5S,6R-diHETE	Cayman Chemicals	Cat#35200
5S,6S-diHETE	Cayman Chemicals	Cat#35210
Critical commercial assays		
Leukotriene B ₄ ELISA kit	Cayman Chemicals	520111
Mouse Myeloperoxidase DuoSet ELISA	R&D systems	Cat#DY3667
EasySep Mouse neutrophil enrichment kit	Stemcell	Cat#19762
Experimental models: Organisms/strains		
<i>Candida albicans</i> SC5314 iRFP	Robert Wheeler	Hopke et al. 2016
<i>Mus musculus</i> C57BL/6J	The Jackson Laboratory	Strain #: 000664
<i>Mus musculus</i> 129S1/SvImJ	The Jackson Laboratory	Strain #:002448
<i>Mus musculus</i> B6.129S2-Alox5 ^{tm1Fuy/J}	The Jackson Laboratory	Strain #:004155
<i>Mus musculus</i> 129-Lta ₄ h ^{tm1Bhk/J}	The Jackson Laboratory	Strain #:004446
Software and algorithms		
FlowJo	NA	https://www.flowjo.com/
ImageJ	NA	https://imagej.nih.gov/ij/
Analyst version 1.7.1	Sciex	https://sciex.com/support/software-support/software-downloads
LibraryView version 1.4	Sciex	https://sciex.com/support/software-support/software-downloads

(Continued on next page)

Continued

REAGENT or RESOURCE	SOURCE	IDENTIFIER
Sciex OS-Q version 1.7.0.36606	Sciex	https://sciex.com/support/software-support/software-downloads
Other		
PolyPico PicoSpotter	NA	https://www.polypico.com/products/
Isolute C18 (100mg/3mL) columns	Biotage	Cat#220-0010-B
Kinetex C18 column (100 mm × 3.0 mm × 2.6 μm, 100Å)	Phenomenex	Cat#00D-4759-Y0
6500+ Triple Quadrupole QTRAP mass spectrometer	Sciex	Cat#5062192C, https://sciex.com/products/mass-spectrometers/qtrap-systems/qtrap-6500plus-system
ExionLC AC System	Shimadzu/Sciex	Cat#5036665, https://www.sciex.com/cr/products/hplc-products/exionlc
Extrahera automated extractor	Biotage	Cat#414001, https://www.biotage.com/automated-solid-phase-extraction

RESOURCE AVAILABILITY

Lead contact

Further information and requests for resources and reagents should be directed to and will be fulfilled by the lead contact, Bryan Hurley (bphurley@mgh.harvard.edu).

Materials availability

This study did not generate any new unique reagents. Slides and plates for the swarming assays are available through the BioMEMS Core at the Massachusetts General Hospital <https://researchcores.partners.org/biomem/about>.

Data and code availability

- All data reported in this article will be shared by the [lead contact](#) on request.
- This article does not report any original code.
- Any additional information required to reanalyze the data reported in this article is available from the [lead contact](#) on request.

EXPERIMENTAL MODEL AND SUBJECT DETAILS

Animals

The following strains of mice were obtained from Jackson Laboratories: wild-type C57BL/6J and S129 (129S1/SvImJ), knockout mice *alox5*^{-/-} (B6.129S2-Alox5^{tm1F_{un}}/J)([Chen et al., 1994](#)) and *Ita4h*^{-/-} (129-Lta4h^{tm1Bhk}/J) ([Byrum et al., 1999](#)). Eight to twenty weeks old male and female mice of different genotypes were used to isolate bone marrow cells. The Institutional Animal Care and Use Committee at Massachusetts General Hospital (MGH) approved the animal protocols used in this study. The mice were housed and bred in the the animal facility of MGH. The laboratory animal care and use program at MGH is accredited by AAALAC International, has an assurance with the Office of Laboratory Animal Welfare (OLAW) and is registered with the United States Department of Agriculture (USDA).

Microbial strains

Candida albicans SC5314 far-red fluorescence expressing strain (SC5314 iRFP) was a kind gift of Robert Wheeler at the University of Maine. ([Hopke et al., 2016](#)) *C. albicans* was inoculated to fresh liquid YPD and grown overnight with shaking at 30°C.

METHOD DETAILS

Isolation of bone marrow cells and purification of bone marrow neutrophils

Bone marrow cells were isolated from C57BL/6, 129S1, *alox5*^{-/-}, and *Ita4h*^{-/-} mice (Jackson Laboratories) as described previously with mild modifications ([Boxio et al., 2004](#)). Briefly, mice were euthanized with CO₂,

and femurs and tibia were flushed with HBSS without calcium and magnesium (Thermo Fisher Scientific). Spicules or bone matrix were removed by 40 μm cell strainer (Fisher). Red blood cells were lysed in cold NH_4Cl lysis buffer as described previously. (Hurley et al., 2004) About $1.5 - 2.5 \times 10^7$ bone marrow cells were isolated per mouse and 26–40% of the bone marrow cells were CD11b+Ly6G+ neutrophils as confirmed by flow cytometry by using fluorescently-labeled antibodies for CD45, CD11b and Ly6G (Thermo Fisher Scientific). The majority of neutrophils (94%) were morphologically mature and functionally competent, as reported previously. (Boxio et al., 2004) This technique allows for rapid isolation of 17-fold more neutrophils than those isolated from peripheral blood per mouse. Additional neutrophil purification was performed using the EasySep mouse neutrophil enrichment kit (STEMCELL), following the manufacturer's recommended protocol. The purity of CD11b+Ly6G+ neutrophils was 65-75% as evaluated by flow cytometry analysis.

Phagocytosis and ROS production during *C. albicans* challenge

Murine neutrophils were harvested from the tibias and femurs of B6 and $\text{alox5}^{-/-}$ mice as previously described (Wang et al., 2006). Briefly, bones were crushed in FACs buffer (2% heat-inactivated fetal bovine serum in PBS), strained through a 40 μm filter, and red blood cells were lysed using 0.2% and 1.6% NaCl solutions. Neutrophils were then harvested by a Ficoll gradient (Histopaque, Sigma Aldrich). To assess phagocytosis and ROS production, neutrophils were co-incubated with a far-red fluorescent protein-expressing *C. albicans* strain (Hopke et al., 2016) at a ratio of 5 yeast cells per neutrophil for 1 h at 37°C in a 1.5-mL tube. Samples were incubated with dihydrorhodamine-1,2,3 (DHR-123 at 1 μM , Life Technologies, Eugene, OR) to assess ROS production for each condition. Where appropriate, neutrophils were treated with 30 μM of cytochalasin-D (Sigma) to inhibit phagocytosis or with LTB_4 (0.6 nM) for phenotype rescue. Following co-incubation, samples were placed on ice and labeled with Ly6G-PE (BioLegend) for 15 min, washed in FACs buffer, and plated in a 96-well U-bottom plate. A BD FACSCeleta Cell Analyzer (BD Biosciences) with a high-throughput plate adaptor running BD FACSDiva Software (v9.0). Percent ROS was measured by selecting doubly positive Ly6G-PE neutrophils and DHR-123 fluorescent cells, whereas percent phagocytosis was measured by fluorescent *C. albicans* in neutrophils. Flow data were analyzed using FlowJo 10 software (FlowJo, Ashland, OR).

Swarming array printing

Utilizing a microarray printing platform (Picospotter PolyPico, Galway, Ireland), we printed a solution of 0.1% poly-L-lysine (Sigma-Aldrich) and ZETAG targets with 100 μm diameter. For microscopy and ELISA experiments, we printed eight by eight arrays in a sixteen-well format on ultra-clean glass slides (Fisher Scientific). For LC-MS/MS experiments, we printed over 4500 targets covering the glass slide. Slides were screened for accuracy and then dried at 40°C for 2 h on a heated block. After 2 h, slides were removed from the heat block and left at room temperature until required.

Patterning of *Candida albicans* cluster targets

Swarming arrays were created as described (Hopke et al., 2020). Briefly, 16-well ProPlate wells (Grace Bio-labs) or single-well ProPlate wells were attached to glass slides with printed arrays of poly-L-lysine/ZETAG. A suspension of the desired target, in this case, live *C. albicans*(SC5314 iRFP) yeast in water, was added to each well (50 μL per well for the 16-well format, 1.5 mL for the single well) and incubated with rocking for 5 min. Following incubation, wells were thoroughly washed out with PBS to remove unbound targets from the glass surface. Wells were screened to ensure appropriate patterning of targets onto the spots with minimal non-specific binding before use.

Swarming experiments

All imaging experiments were conducted using a fully automated Nikon TiE microscope. Time-lapse imaging was conducted using a 10x Plan Fluor Ph1 DLL (NA = 0.3) lens, and endpoint images were taken with a 2x Plan Apo (NA = 0.10) lens. Swarming targets (*C. albicans* clusters) to be observed during time-lapse were selected and saved using the multipoint function in NIS elements prior to loading of cells. Bone marrow cells or enriched bone marrow neutrophils were stained with Hoechst (Thermo Fisher Scientific) and resuspended in IMDM with 20% FBS (Thermo Fisher Scientific). 500,000 cells were added to each well for individual genotype conditions. 250,000 cells each were added in mixed genotype conditions. All selected points were optimized using the Nikon Perfect Focus System before launching the experiment. In experiments using chemical inhibitors, neutrophils were pre-incubated with the chemical or

appropriately matched vehicle control for 30 min before use. The supernatants were collected 2 h after the cells were added and saved at -80°C after removing the cells by centrifugation.

Image analysis

Area analysis was performed manually by outlining the swarms or areas of fungal growth in the NIS-elements (v4.00.12; Nikon Inc) or FIJI (FIJI is just ImageJ v2.0.0-rc-59/1.52p, NIH) software. For the area of the swarm, only the swarm itself (just the immune cells) was measured. This was done using the DAPI fluorescent channel image, using Hoechst staining to identify neutrophils. For areas of fungal growth, a combination of brightfield and fluorescent channels was used. Fungi used in experiments were always far-red fluorescent (Hopke et al., 2016). We combined the appropriate fluorescent channel with the brightfield image to be sure we included any escaped fungal elements, like lone hyphae, that may not show up well in the fluorescent channel.

Bone marrow cell culture

Bone marrow cells from single or mixed cell types were seeded in 96-well round-bottom tissue culture plates at $200\ \mu\text{L}/\text{well}$ with 5×10^6 cells/mL. Cells were incubated with calcium ionophore A23187 (Sigma-Aldrich) at $20\ \mu\text{g}/\text{mL}$ at 37°C with $5\% \text{CO}_2$ for 1 h. Cells were removed by centrifugation at $500 \times g$ for 5 min. The supernatants were saved at -80°C for LTB_4 ELISA assays.

LTB_4 quantification by ELISA

Supernatants from the swarming assay for each condition were collected at the indicated time points and subjected to a competitive LTB_4 ELISA (Cayman chemical) according to the manufacturer's protocol. Briefly, $50\ \mu\text{L}$ LTB_4 standards diluted in 1:2 series and supernatants from the swarming assay were added to the 96-well plate precoated with mouse anti-rabbit IgG and incubated with LTB_4 antiserum and AChE linked to LTB_4 (tracer) at 4°C overnight. The plate was then washed five times with wash buffer, followed by incubation with Ellman's reagent for 90–120 min. The absorbance at 405 nm was measured by SpectraMax iD5 microplate reader (Molecular Devices). The readings of diluted standards were plotted as $\log \text{it B}/\text{B}_0$ versus $\log \text{LTB}_4$ concentration using a linear fit and were used to determine sample LTB_4 concentrations according to the manufacturer's instructions.

BLT1 receptor quantification on mouse neutrophils

Bone marrow cells isolated from C57BL/6, $\text{alox5}^{-/-}$, S129, and $\text{Ita}_4\text{h}^{-/-}$ mice were applied to LIVE/DEAD fixable Dead Cell staining by incubating with Near-IR fluorescent reactive dye (Thermo Fisher Scientific) in HBSS at room temperature for 15 min in the dark, followed by two washes with HBSS. The cells were then resuspended in eBioscience™ Flow Cytometry staining buffer (Thermo Fisher Scientific) and incubated with rat anti-mouse CD16/CD32 monoclonal antibody on ice for 10 min to block the Fc receptor. The following antibodies were then added to stain the cells on ice for 15 to 30 min in the dark: PE-conjugated rat anti-mouse CD45 (BioLegend), PerCP-Cyanine5.5-conjugated rat anti-mouse CD11b (Thermo Fisher Scientific), APC-conjugated rat anti-mouse Ly-6G (Thermo Fisher Scientific), Alexa Fluor 488-conjugated rabbit anti-mouse BLT1 (Bioss Antibodies). The cells were washed and applied to flow cytometry analysis using Attune NxT Flow Cytometer (Thermo Fisher Scientific). The data were analyzed by FlowJo. Neutrophils were gated as $\text{CD45}^+\text{CD11b}^+\text{Ly-6G}^+$ live cells and the mean fluorescence intensity (MFI) of BLT1 on neutrophils was compared between C57BL/6, $\text{alox5}^{-/-}$, S129, and $\text{Ita}_4\text{h}^{-/-}$ genotypes.

Chemotaxis assay

The chemoattractive activity of the supernatants obtained from swarming experiments was measured by performing a bone marrow cell transmigration assay using 96-well Transwell with a pore size of $3\ \mu\text{m}$ (Corning). Bone marrow cells were isolated from the femoral and tibial bones of C57BL/6J $\text{alox5}^{-/-}$ or $\text{Ita}_4\text{h}^{-/-}$ mice, as described above. One hundred microliters of supernatant were added to the bottom well, and 10^6 bone marrow cells in $75\ \mu\text{L}$ HBSS were added to the inside of the Transwell insert. After incubation at 37°C for 2 h, the inserts were removed. Bioactivity was determined by the number of neutrophils that migrate through the Transwell towards the conditioned swarming supernatant or LTB_4 ($0.2\ \text{ng}/\text{mL}$). Moreover, MPO assay was performed with the cells migrated to the bottom wells as described previously (McCormick et al., 1995).

Targeted liquid chromatography-tandem mass spectrometry metabololipidomics

Bone marrow cells (20×10^6 cells/group) from *alox5*^{-/-}, *Ita4h*^{-/-}, *alox5*^{-/-} + *Ita4h*^{-/-}, C57BL/6J wild-type, or 129S1 wild-type suspended in 2 mL IMDM (phenol red free) containing 0.1% human serum albumin were incubated for 2 h at 37°C in glass slides/wells covered in large arrays of *C. albicans* clusters (100 μm in diameter). The incubations were quenched with 2 mL 100% ice-cold LC-MS grade methanol (Thermo Fisher Scientific, Waltham, MA, USA) containing 500 pg d₄-LTB₄ (Cayman Chemicals, Ann Arbor, MI, USA) for calculating recovery and quantity of endogenous materials. Protein was precipitated by storage at -80°C for a minimum of 30 min, followed by centrifugation at 1000 ×g for 10 min at 4°C. Supernatants were extracted using an automated extractor (Extrahera, Biotage, Charlotte, NC, USA) by solid phase extraction on 100 mg C18 columns (Biotage) as described in (Shay et al., 2021). LTB₄ and its isomers (6-trans-LTB₄, 6-trans-12-epi-LTB₄, 5S,6S-diHETE, and 5S,6R-diHETE) were eluted with spectrophotometric grade methyl formate (Sigma-Aldrich). Samples were evaporated under a gentle stream of nitrogen gas and immediately resuspended in a LC-MS grade methanol-water mixture (50:50, v/v) for analysis by a 6500+ Triple Quadrupole QTRAP mass spectrometer in low mass and negative polarity mode (Sciex, Framingham, MA, USA) equipped with an ExionLC (Shimadzu, Kyoto, Japan). A Kinetex C18 column (100 mm × 3.0 mm × 2.6 μm, 100 Å, Phenomenex) was maintained at 50°C in a column temperature-controlled oven.

LTB₄ and its isomers (6-trans-LTB₄, 6-trans-12-epi-LTB₄, 5S,6S-diHETE, and 5S,6R-diHETE) were quantified using targeted multiple reaction monitoring (MRM) with the following settings: Q1 (*m/z*) = 335.2, Q3 (*m/z*) = 195.1 or 115.1 (diHETEs), declustering potential = -40 V, entrance potential = -10 V, collision energy = -22 V, and collision cell exit potential = -12 V. The data were acquired with Analyst version 1.7.1 (Sciex) and analyzed with, and screen captured from Sciex OS-Q version 1.7.0.36606 (Sciex). The LTB₄ calibration curve was used for quantification and had a correlation coefficient (*r*²) of 0.99742. The solvents, gradient, MRM, and enhanced product ion (EPI) mode settings are detailed in (Shay et al., 2021). Each mediator was identified by a matching retention time, and an unbiased MS/MS library fit (≥70%) to synthetic materials, as well as the presence of key structural fragments. The synthetic materials in the custom metabololipidomics library were validated against authentic materials and was created using LibraryView version 1.4 (Sciex). The following library smart confirmation search parameters were used for the identification of LTB₄ and its isomers: precursor mass tolerance ±0.8 Da, fragment mass tolerance ±0.8 Da, collision energy ±5 eV, use polarity, an intensity threshold of 0.02, a minimum purity of 5.0%, and an intensity factor of 100.

QUANTIFICATION AND STATISTICAL ANALYSIS

All statistics were conducted using GraphPad Prism 7.03 software. Data were tested for normality using a D'Agostino-Pearson omnibus normality test. Normally distributed data were analyzed with Student's T-test or One Way ANOVA with Tukey's post-test. Non-normally distributed data were analyzed with a Mann-Whitney or Kruskal-Wallis with Dunn's post-test where appropriate. Statistical significance was considered for *p* < 0.05 and is provided in the relevant figure legends. Error bars represent standard deviation unless otherwise indicated.